

Iteratively Reweighted Least Squares for Maximum Likelihood Identification of Synchronous Machine Parameters from On-line Tests

R. Wamkeue, (StM)
École Polytechnique,
Montréal, QC, Canada

I. Kamwa, (M)
Hydro-Québec,
Montréal, QC, Canada

X. Dai-Do, (SM)
École Polytechnique,
Montréal, QC, Canada

A. Keyhani, (SM)
Ohio State University,
Columbus, Ohio, USA

Abstract - This paper presents a new approach for the statistical identification of synchronous-machine parameters from on-line test data that were recorded on a 202-MVA hydro-generator at Hydro-Quebec's La Grande 3 generating station. Data processing is performed to remove harmonics in noise-corrupted measurements. The time-domain parameter identification is carried out by means of our proposed maximum-likelihood estimation method, also called the iteratively reweighted least-squares algorithm. A comparison of the results with the ordinary weighted least-squares estimation, which is equivalent to the maximum-likelihood estimation only when the noise is white, shows the superiority of the proposed method. This procedure appears more convenient than previous schemes for parameter identification of the synchronous-machine linear equivalent-circuits, especially when the noise statistics are poorly known.

I. Introduction

Although standstill testing in the time and frequency domains has gained rapid popularity, owing to the simplicity of its implementation even on very large machines, it is still sometimes criticized for its excessively low levels of test currents, not to mention that the rotational effects of the coupling axes, the centrifugal force effects on damper windings and the magnetic saturation effects cannot be observed during standstill [1, 2]. These limitations triggered the emergence of running time-domain response (RTDR) testing, based on small [3] or large [4] signal disturbances around an operating point.

The maximum-likelihood estimator has been extensively used for synchronous-machine parameter identification from frequency and time-domain response data [3], [5, 6]. Despite the quality of the results obtained by many authors using this estimator, the adequacy of its application remains questionable.

The purpose of this work is to present a new approach to maximum-likelihood identification of the synchronous-machine parameters from time-domain on-line large-disturbance test, obtained by abruptly changing the reference voltage. The estimation method is derived from the generalized least-squares estimator. This technique provides accurate estimates and appears as the best choice to avoid the shortcomings of the classical formulation of the maximum-likelihood estimation.

PE-191-EC-0-12-1997 A paper recommended and approved by the IEEE Electric Machinery Committee of the IEEE Power Engineering Society for publication in the IEEE Transactions on Energy Conversion. Manuscript submitted July 1, 1997; made available for printing December 12, 1997.

II. Parametrization of generalized models

Estimation of the equivalent circuits in Fig.1 consists in determining the following parametric vector of reactances and resistances (per units) for given integers n_d , n_q and ω_n :

$$\theta_s^T = \left[\mathfrak{R}_d \quad \mathfrak{R}_q \quad \chi_d \quad \chi_q \quad \chi_m \right] \quad (1)$$

$$\mathfrak{R}_d = \begin{bmatrix} r_a & r_f & r_{D_i} \end{bmatrix}; \chi_d = \begin{bmatrix} x_a & x_f & x_{D_i} \end{bmatrix}; i = 1 \dots n_d \quad (2)$$

$$\mathfrak{R}_q = \begin{bmatrix} r_a & r_{Q_j} \end{bmatrix}; \chi_q = \begin{bmatrix} x_a & x_{Q_j} \end{bmatrix}; j = 1 \dots n_q \quad (3)$$

$$\chi_m = \begin{bmatrix} x_{md} & x_{mq} & x_{kf_1} & \dots & x_{kf_{nd}} \end{bmatrix} \quad (4)$$

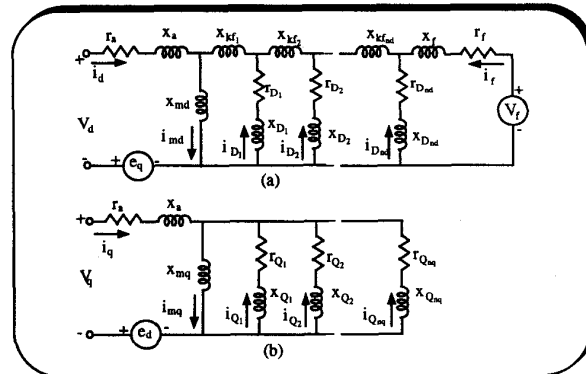


Fig.1: Generalized equivalent circuit of the synchronous machine: (a) $e_d = \omega_m \Psi_d$; (b) $e_q = -\omega_m \Psi_q$

In the present study, the input-output data originate from normal operating records, with a machine running in a sufficiently informative mode (section IV). The outputs $y(k)$ can be sampled

at intervals $\{t_k = t_0 + k\tau; k = 0, 1, \dots, N\}$ by means of an experimental test bed. The data acquisition system inevitably introduces stochastic perturbations on both the process $\{n(k)\}$ and the measurements $\{m(k)\}$. Therefore, in the discrete-time state space representation of the machine, the dependence on the unknown parameter vector $\theta = \begin{bmatrix} \theta_s^T & \theta_n \end{bmatrix}$ can be explicitly expressed as follows:

$$\begin{aligned}
x_0 &= x(0) \\
x(k+1, \theta) &= A(k, \theta)x(k, \theta) + B(k, \theta)u(k) + F(k, \theta)n(k, \theta) \\
y(k, \theta) &= Cx(k, \theta) + Du(k) + G(k)m(k) \\
w_l[\theta, x(k, \theta); u(k)] &\geq 0, l = 1, 2, \dots, \lambda;
\end{aligned} \tag{5}$$

$$A(k, \theta) = e^{A(\theta_s)\tau}; \quad B(k, \theta) = \begin{pmatrix} \tau A(\theta_s)^T \\ \int_0^\tau e^{A(\theta_s)(\tau-T)} dT \end{pmatrix} B(\theta_s) \tag{6}$$

with the following covariance matrices.

$$E[n] = 0; \quad Q = E[nn^T]; \quad E[m] = 0 \tag{7}$$

$$R_0 = E[mm^T]; \quad E[x(0)] = 0; \quad P_0 = E[xx^T] \tag{8}$$

where $x \in \mathfrak{R}^r$, $u \in \mathfrak{R}^m$, $y \in \mathfrak{R}^z$ are in order, the state, input and output vectors with $q = 3n_d + 2n_q + 5$, $r = n_d + n_q + 3$ and $\theta_s \in \mathfrak{R}^q$. The state variables in (5) are a function not only of the system-machine parameter vector θ_s but also of the noise parameter vector θ_n . The w_l are λ equality and inequality constraints relating a priori x , u and θ_s , and may serve as stability bounds. The system state matrices $A(\theta_s)$, $B(\theta_s)$, C and D are given in appendix. Q and R_0 are constant but unknown noise covariance matrices.

III. The maximum-likelihood estimator

The maximum likelihood estimate θ_M is the value of θ which maximizes the joint probability that $y(k, \theta)$ is equal to the actual measurements in hand [7, 8]. This is equivalent to minimizing the negative logarithm of (9), to conform with optimization conventions.

$$\begin{aligned}
V(\theta) &= \frac{1}{2} \sum_{k=1}^N \left(\varepsilon(k)^T R(\theta)^{-1} \varepsilon(k) \right) + \frac{1}{2} N \log(\det(R(\theta))) \\
\varepsilon &= y - y_p; \quad R(\theta) = E[\varepsilon\varepsilon^T]
\end{aligned} \tag{10}$$

where ε is the innovation sequence, R the corresponding covariance matrix and y_p is the predicted value of the measured output vector y . Rigorously, in the estimation procedure, the unknown process covariance matrix Q and the innovation sequence covariance matrix R should be identified at the same time as the system-parameter vector so that, by the end of this procedure, *the noise becomes white* for the optimal value of R and Q [7-10]. Otherwise, if R is a fixed known matrix, (9) could be one of the following estimators [8]:

1. If $R = C^{te}$ is the known covariance matrix of the residuals, (9) is the Markov estimator.
2. If $R = C^{te}$ is an arbitrary fixed matrix, (9) is the well known weighted least-squares estimator.
3. If $R = C^{te} = I$ is the identity matrix, (9) is the ordinary least-

squares estimator.

III.1 Shortcomings of previous approaches to the maximum likelihood identification of synchronous machines

In the approaches developed in [3, 5, 6], for instance, R is obtained from a Kalman filter according to (11);

$$R(k) = R_0 + CP_e(k)C^T \tag{11}$$

where P_e is the estimated covariance matrix of the state vector.

However, such an approach has the following shortcomings:

- The method used to determine the a priori unknown Q matrix is not always clear.
- The above formulation is restrictive and cannot compute machine parameters when perfect (noise-free) measurements are assumed for all the system state variables; i.e. if in (5): $G = 0$, $R_0 = 0$, $D = 0$, then, according to (9) and (11), C needs to be non-singular. Unfortunately, since the machine damper windings are not accessible to observation, C is never of full rank and the previous method cannot be applied.
- The optimum results of Kalman filtering require an exact knowledge of the process and measurement noise covariance matrices Q and R [9]. In this sense, nothing shows that the Kalman filter as used in the previous formulation works optimally. For example, knowing that no restriction on using the above procedure is mentioned by the authors, let us suppose a stochastic environment where process noise can be neglected, $F = 0$ in (5) and $P = P_e = 0$ in (11); hence $R(k) = R_0$ is an arbitrary fixed value and (9) becomes

$$L(\theta) = \frac{1}{2} \sum_{k=1}^N \left(\varepsilon(k)^T R_0^{-1} \varepsilon(k) \right) \tag{12}$$

which is basically the well known *weighted least-squares estimator* previously defined. In this case, and more generally, when the process noise covariance matrix Q is arbitrary fixed to an a priori value as in [3, 5, 6], the maximum-likelihood procedure based on (9), becomes mathematically equivalent to the *weighted least-squares estimation* (WLS).

III.2 New approach of maximum-likelihood estimation: the iteratively reweighted least-squares algorithm

The generalized least-squares estimate θ_G is the value of θ that minimizes the quadratic functional defined by [11]:

$$M(\theta) = \sum_{k=1}^N \varepsilon(k)^T R(\theta)^{-1} \varepsilon(k) \tag{13}$$

The matrix R in (13) is also unknown, but it may be observed that if R could be estimated at each iteration i of the identification procedure, (9) and (13) in terms of the optimization criterion, will be equivalent. In other words, the generalized least-squares estimate of θ is equal to its maximum-likelihood estimate ($\theta_G = \theta_M$). It is well proved that at θ_G , the best estimate of the innovation covariance matrix, R is given by [7, 11, 12].

$$R(\theta) = \frac{1}{N} \sum_{k=1}^N \varepsilon(k) \varepsilon(k)^T \quad (14)$$

The problem of the generalized least squares can thus be solved by the following three-step procedure [11]:

1. Set $R(\theta) = I$ and minimize (13) with respect to θ .
2. Compute $R(\theta)$ from (14) using the residuals from step 1.
3. Form the cost function (13) using the value of $R(\theta)$ calculated from step 2 and solve the minimization problem.

Steps 2 and 3 are repeated until convergence is attained. At each iteration i of step 2, $R_i(\theta)$ is updated by (14); thus (13) behaves like the weighted least squares that will be *iteratively reweighted* during future iterations, since $R_i(\theta) \neq R_j(\theta)$ for two distinct iterations i and j . In the exact maximum likelihood method, this procedure is applied by simply changing equation (13) for equation (9) in steps 1 and 3. The predicted state and output variables are then computed using the discrete form (15) obtained by combining the discrete deterministic state-space model of the system with the Kalman prediction-correction formulation [13];

$$\begin{aligned} x_p(k+1, \theta) &= [A(k, \theta) - KC]x_p(k, \theta) \\ &\quad + [B(k, \theta) - KD \quad K] \begin{bmatrix} u(k) \\ y(k) \end{bmatrix} \quad (15) \\ y_p(k, \theta) &= Cx_p(k, \theta) + \begin{bmatrix} D & O_{1,z} \end{bmatrix} \begin{bmatrix} u(k) \\ y(k) \end{bmatrix} \end{aligned}$$

where the indices p denote the predicted variable values, and $O_{1,z}$ is $1 \times z$ zero matrix; K is the limiting (steady-state) Kalman gain matrix defined in (16). This choice offers the advantage of reducing computation time and ensuring that the filter is asymptotically optimal. Since $K(k) \rightarrow K$ as $k \rightarrow +\infty$, the state prediction error $P(k) \rightarrow P$ as $k \rightarrow +\infty$; thus P would satisfy the Riccati matrix equation (17). The covariance matrix of the discretized process noise Q is obtained from (18), [7].

$$K = PC^T(R + CPC^T)^{-1} \quad (16)$$

$$P = (e^{A\tau}) [P - KCP + Q] (e^{A\tau})^T \quad (17)$$

$$Q = \int_0^\tau e^{-A\sigma} FF^T e^{-A^T\sigma} d\sigma \quad (18)$$

In practice, $Q = \tau FF^T$; the previous approximation of Q is such that τ must be small compared to the system time constants for good estimation. Since F is unknown, an adequate value Q_0 of Q is chosen to initialize the Kalman Filter. Further estimates of Q which the entries are the elements of θ_n ($Q = \text{diag}(\theta_n)$), are computed together with the system parameter vector θ_s . At each iteration, the update value of Q is introduced in (17).

Since R is estimated by (14), it is completely independent of Q . At the end of the procedure, when an optimal value of Q is obtained, F is deduced from (18). This formulation is still valid when a process noise model is avoided or when perfect measurements are assumed. In the aim to show the effectiveness of the present work, the proposed *maximum-likelihood estimation* formulation (MLE) also called *the iteratively reweighted least-squares algorithm*, is implemented at the same time with the *weighted least-squares estimation* (WLS) procedure normally equivalent to the classical maximum-likelihood estimation as previously established in section III.1.

A consistent weighted least-squares estimator can be derived from (12) by replacing R_0 with $W = \frac{R_0}{N}$; ($N \rightarrow +\infty$). The implementation of these two estimation procedures ((MLE) and (WLS)) is completed by choosing a suitable constrained optimization algorithm as developed in the reference [15]. In order to ensure the Kalman filter stability, Q must be semidefinite positive, and R should be definite positive to be physically meaningful.

IV. Experiment setup

The test report [16] covers many tests done in spring 1993 on the Hydro-Québec network under normal operating conditions. The experimental arrangement of the tests is shown in Fig. 2. The machine under test is a wye-connected hydro turbine-generator at La Grande 3, rated at 202 MVA, 13.8 kV, 0.95 power factor, 60 Hz and 64 poles with a synchronous speed of 112.5 rpm. Two tests were selected for this study. The identification on-line test was performed by introducing a large disturbance in the machine excitation reference voltage. The step response is obtained using a pulse voltage of 15% for 6 cycles of the fundamental. This type of test has the advantage of being influenced by the machine saturation. The second test selected is for the cross-validation of the identified models. For this purpose, measured terminal and field voltages are directly used as input signals in the simulation. Comparisons are then made between the measured and simulated variables.

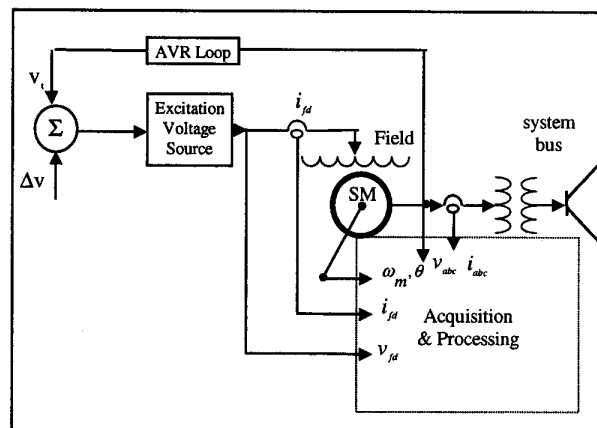


Fig. 2: On-line testing using field voltage perturbations.

V. Data preprocessing

The data derived from the previous tests are very noisy, as illustrated by the field current in Fig. 3 (a). Each test contains 60,000 points/signal. The noise is probably due to the surrounding electromagnetic interference, sensor noise, and the rectification voltage process of the excitation system. The filtered field current is shown in Fig. 3 (b). Two important stages of data processing are needed.

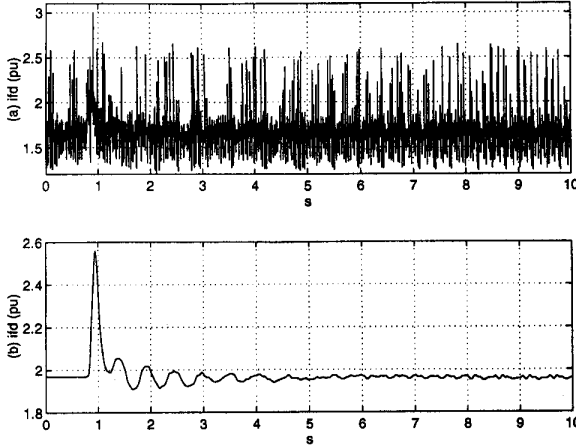


Fig. 3: Raw and smoothed field current.

V.1 Compression and smoothing

This first stage consists in using the Clarke transformation [17] to derive the fundamental variables V, I, P and Q with a decimation of 1:13 order aim to obtain a final signal of 240 Hz. The Clarke transformation of a given three-phase system (g_a, g_b, g_c) is obtain by

$$\begin{bmatrix} g_\alpha(t) \\ g_\beta(t) \\ g_0(t) \end{bmatrix} = \sqrt{\frac{2}{3}} \begin{bmatrix} 1 & \frac{1}{\sqrt{3}} & -\frac{1}{\sqrt{3}} \\ 0 & \frac{2}{\sqrt{3}} & \frac{2}{\sqrt{3}} \\ \frac{1}{\sqrt{2}} & \frac{1}{\sqrt{2}} & \frac{1}{\sqrt{2}} \end{bmatrix} \begin{bmatrix} g_a(t) \\ g_b(t) \\ g_c(t) \end{bmatrix} \quad (19)$$

The terminal voltages and currents space-phasors, also known as the positive symmetrical instantaneous components are defined by (20), while the machine power swings are given by (21).

$$v_{cl}(t) = v_\alpha(t) + jv_\beta(t); \quad i_{cl}(t) = i_\alpha(t) + ji_\beta(t) \quad (20)$$

$$s_{cl}(t) = v_{cl}(t)i_{cl}(t)^* = p_{cl}(t) + jq_{cl}(t) \quad (21)$$

where g^* denotes the conjugate complex of g . The phasors $v_{cl}(t)$ and $i_{cl}(t)$ contain all the necessary information to describe the positive and negative sequences at all harmonic frequencies of the terminal voltages and currents. These previous phasors are therefore particularly suitable for efficiently defining the true rms and average values of terminal variables [17]; thus

$$I = \sqrt{\frac{1}{T} \int \frac{1}{T^3} (i_{cl} i_{cl}^*) dt}; \quad V = \sqrt{\frac{1}{T} \int \frac{1}{T^3} (v_{cl} v_{cl}^*) dt} \quad (22)$$

$$P = \frac{1}{T} \int (p_{cl}(t)) dt; \quad Q = \frac{1}{T} \int (q_{cl}(t)) dt; \quad (23)$$

The procedure to evaluate (22,23) consists in using a low-frequency multirate filter whose passband depends on the actual application. This technique is efficient for rejecting second order harmonics and is insensitive to large frequency variations. The decimation process is inspired by reference [18].

V.2 Rotor angle and Park transformation

For the saturated steady state, the rotor angle δ_0 and the other Park component variables are computed from equation (24-27) [19, 20].

$$\delta_0 = a \tan \left(\frac{x_{qs} I \cos(\phi) + r_a I \sin(\phi)}{V + r_a I \cos(\phi) - x_{qs} I \sin(\phi)} \right) \quad (24)$$

$$i_d = I \sin(\delta_0 - \phi); \quad i_q = I \cos(\delta_0 - \phi) \quad (25)$$

$$v_d = V \sin(\delta_0); \quad v_q = V \cos(\delta_0) \quad (26)$$

$$i_{fd}^c = \frac{v_q - e_a i_q - \varepsilon \left(x_a + x_{m ds} (i_{fd}) \right) i_d}{x_{m ds} (i_{fd})}; \quad v_{fd} = r_f i_{fd} \quad (27)$$

$$\frac{|i_{fd}^c(i+1) - i_{fd}|}{i_{fd}} \times 100 \leq 5 \quad (28)$$

In (24), the only uncertainty in computing δ_0 comes from the saturated q -axis reactance x_{qs} ; for a given sample $i = 1, 2, \dots, \gamma$, x_{qs} is adjusted iteratively by establishing that the value of the computed field current i_{fd}^c (27) will be the same as the measured one. A criterion for the steady-state validation conditions could then be defined by (28). For the transient Park components, the rotor angle in the dynamic state should be evaluated because measured data are not available. Krause [21] suggests that for a given space-phasor $g_{cl}(t) = g_\alpha(t) + jg_\beta(t)$, the Park components in the dynamic state are defined by

$$\begin{bmatrix} g_d \\ g_q \end{bmatrix} = \begin{bmatrix} \cos(\delta) & -\sin(\delta) \\ \sin(\delta) & \cos(\delta) \end{bmatrix} \begin{bmatrix} g_\alpha \\ g_\beta \end{bmatrix} \quad (29)$$

$$\delta(t) = \int_0^t 2\pi [f_r(\zeta) - f_s(\zeta)] d\zeta + \delta_0 \quad (30)$$

where f_s and f_r are respectively the synchronous frequency and the rotor speed. Unfortunately, the recorded rotor speed data are not available but it can be well approximated by the frequency of the phasor

$$\bar{e}_q = \bar{v}_t + (r_a + jx_{qs})\bar{i}_t \quad (31)$$

\bar{e}_q is tied to the synchronous-machine internal voltage [21] whose frequency is equal to the rotor speed. \bar{v}_t and \bar{i}_t are phasors of the terminal voltage and current. $\delta(t)$ is then computed by the following procedure:

1. Estimate f_s
2. Estimate f_r
3. Integrate (30) using a digital integrator

The computed initial-condition values are indicated in Table 1. Of the values given for any variable in this table, the first corresponds to the identification test, the second to the cross-validation test. Superscripts c and m indicate computed and measured values respectively.

Table 1: Initial conditions

E_q^m	1.1290 1.1712	I^m	0.8799 0.6103	P^m	0.9356 0.7146	Q^m	-0.3337 0.0128	PF	0.9493 0.9235
v_d^c	0.6008 0.3685	v_q^c	0.9559 1.1013	i_d^c	0.1908 0.2179	i_q^c	0.8590 1.1120	x_{ds}	1.0581 1.0347
δ_0^c	32.1490 19.8920	i_{fd}^m	1.3558 1.4992	i_{fd}^c	1.3488 1.5876	v_{fd}^m	0.0007 0.0011	x_q	0.7000 0.7000

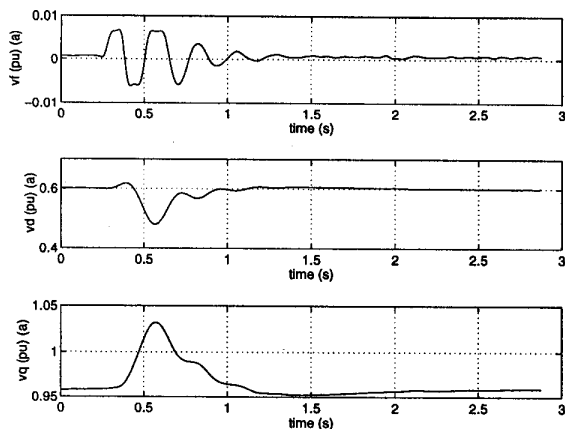


Fig. 4: Smoothed input voltages for the identification procedure.

In both steady-state and transient analysis, the so-called constant model saturation method is used to incorporate magnetic saturation in the machine model. It bases on the assumption that the saturation does not change much during the test. The saturated magnetic reactances $x_{m ds}$ and $x_{m qs}$ obtained from the initial steady-state conditions will therefore be maintained for the transient study. Apart from the peak due to sudden impulse in the field voltage, this assumption is realistic since, the whole behavior of the machine is a disturbance around the initial steady state. The per unit base variables obtained with the method developed in [19] are $V_b=11.268$ (kV), $I_b=11.952$ (kA),

$I_b=848.232$ (A), $V_b=23.814$ (kV).

VI. Results

The computed steady-state conditions are given for the selected tests in Table 1. The machine under test is a salient-pole machine; thus, as suggested in IEEE-Std.1110 [22], the model structure selected needs only one damper winding per axis. The initial equivalent-circuit parameters (Std-M. in Table 2) are calculated from short-circuit time constants graphically obtained using combined Salvatore [24] and Canay [25] algorithms. The dynamic constants of Table 3 are computed from given or estimated equivalent-circuit parameters by the method suggested in [23].

Table 2: Estimated equivalent-circuit parameter values

$\theta_{se}^{(i)}$	x_{kf1}	r_f	r_{D1}	r_{Q1}	x_a
MLE	0.028497	0.0005045	0.0036763	1.6190	0.198
WLS	0.096182	0.0004845	0.0042226	1.6190	0.198
Std-M.	0.0036758	0.00043632	0.0040965	1.6190	0.198
$\theta_{se}^{(i)}$	x_f	x_{D1}	x_{Q1}	x_{md}	x_{mq}
MLE	0.021172	-0.005618	3.8348	0.84987	0.5030
WLS	0.020237	-0.009125	3.8348	0.84987	0.5030
Std-M.	0.011977	0.0033333	3.8348	0.906	0.502
$\theta_{ne}^{(j)}$	x_f	x_{D1}	x_{Q1}	x_{md}	x_{mq}
	0.00001♀	0.00001♀	0.00001♀	0.00001♀	0.00001♀
	0.0000649	0.00007473	0.00009	0.000007	0.000008
diag(R)	initial	0.001	0.001	0.001	
	final	0.000017	0.000098	0.00003	

♀ initial values of the Q matrix diagonal terms

Table 3: Derived dynamic reactance and time-constant estimates

	MLE	WLS	Std-M		MLE	WLS	Std-M.
x'_d	0.3885	0.4054	0.325	T'_d	2.4281	2.6061	1.5848
x''_d	0.2532	0.2766	0.229	T''_d	0.0702	0.06304	0.06716
x'_f	0.3446	0.3725	0.2713	T'_{d0}	6.6133	6.7839	5.4584
x''_f	0.2062	0.1929	0.197	T''_{d0}	0.1068	0.09172	0.09002
x''_q	0.6427	0.6427	0.2125	T''_q	0.00651	0.00651	0.06037
T''_{q0}	0.0071	0.0071	0.1997	T'_f	0.4434	0.44587	0.36914
T''_f	0.0625	0.0596	0.0616	T''_{f0}	0.10012	0.10546	0.08085
T'_{f0}	1.5471	1.4998	1.5315	T_{D1}	-0.0021	-0.0057	0.00224

The input signals to be applied to the model are given in Fig. 4. The consistent weighted least-squares (WLS) estimator (equivalent of classical maximum-likelihood estimation) was implemented in aim to establish a comparison with the proposed maximum-likelihood method (MLE). The oscillographs of Fig. 5-8 illustrate the performance of MLE compared to WLS. They also confirm the consistency of MLE. The identified model is strongly competitive as shown by these figures. It can be observed in Fig. 5-6 that, apart from peak, the identified and the test curves are similar. The components of the estimated parameter vector θ_{se} are listed in Table 2 together with the estimated noise.

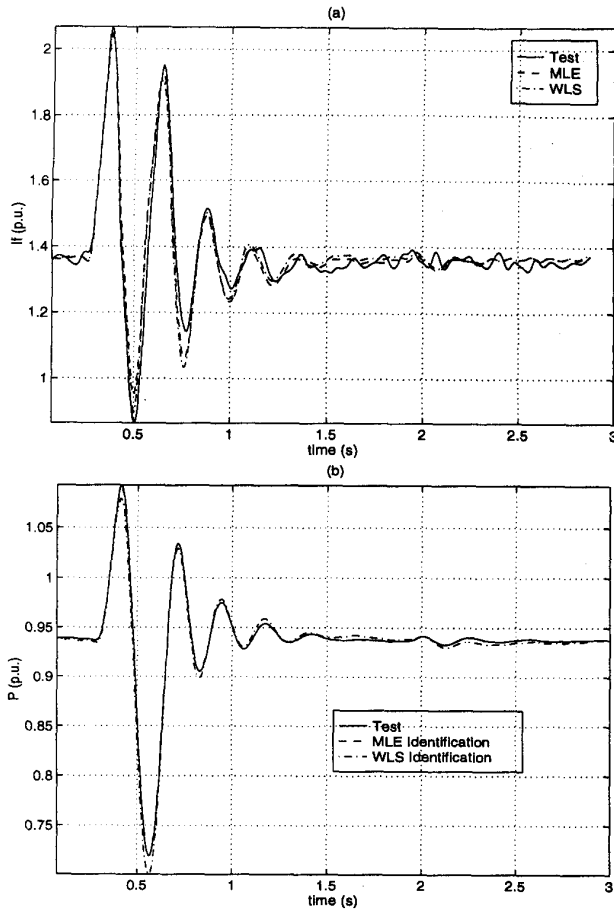


Fig. 5: Synchronous-machine model validation: field current and active power.

parameter vector θ_{ne} . For Kalman filtering, the initial value of the state noise parameter j , is $\theta_n(j) = 10^{-5}$ (Table 2). Fig. 7 shows the various steps in the identification procedure. At first as illustrated by the dotted line (first-stage innovations), the innovation sequence is not white but, by the end of the procedure when the optimal parameter vector is obtained, the residuals become negligible and nearly white, as shown by the full line in Fig. 7 (second-stage innovations) and the final value of innovation covariance matrix R (Table 2). Since the exact values of the machine parameters are unknown, only computation of the confidence regions (Cramer-Rao bounds), not included in this work, could help to appreciate the discrepancy between estimated and unknown true parameters. Nevertheless, the final, nearly white residuals of Fig. 7 and the cross-validation given in Fig. 8 confirm the accuracy of the proposed La Grande 3 machine model for transient analysis around an operating point. The negative value obtained for the d -axis damper winding was also reported by Canay [25] for a turbine-generator. It is an algebraic quantity showing the flux direction in the winding. In addition, the positive Canay reactance estimated or calculated is due to iron saturation.

Interesting insights into the Kalman filter can be derived from the cross-validation analysis given in Fig. 8. Iron saturation for the

cross-validation test and the identification test is different; since the estimated parameters of Table 2 are used for cross-validation, the saturation levels of the identification test and the cross-validation test of the machine represented by reactances $x_{m_{ds}}$ and $x_{m_{qs}}$, are different. This problem is illustrated by the WLS plot in Fig. 8. Otherwise, the Kalman filter of MLE considers this problem as an added noise which is automatically filtered.

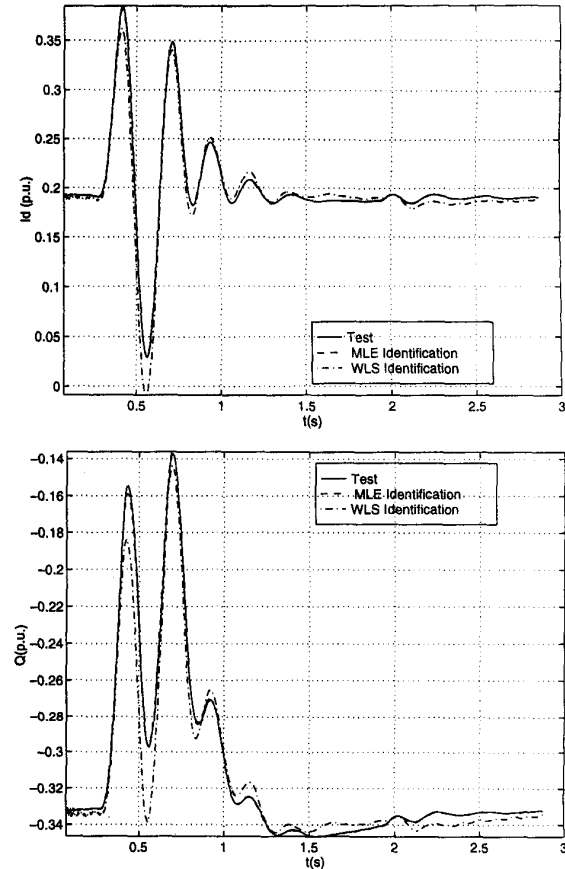


Fig. 6: Synchronous-machine model validation (cont.): d-axis current, and reactive power.

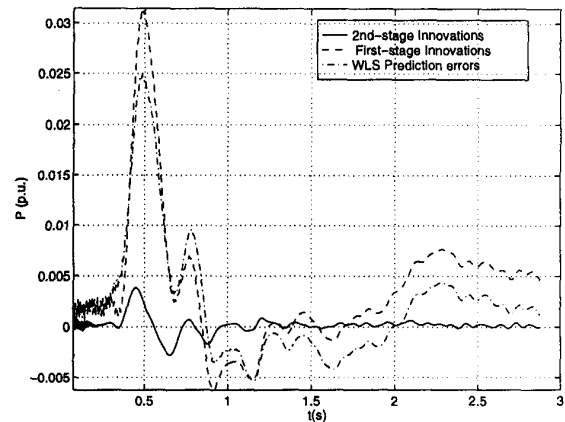


Fig. 7: Model innovations

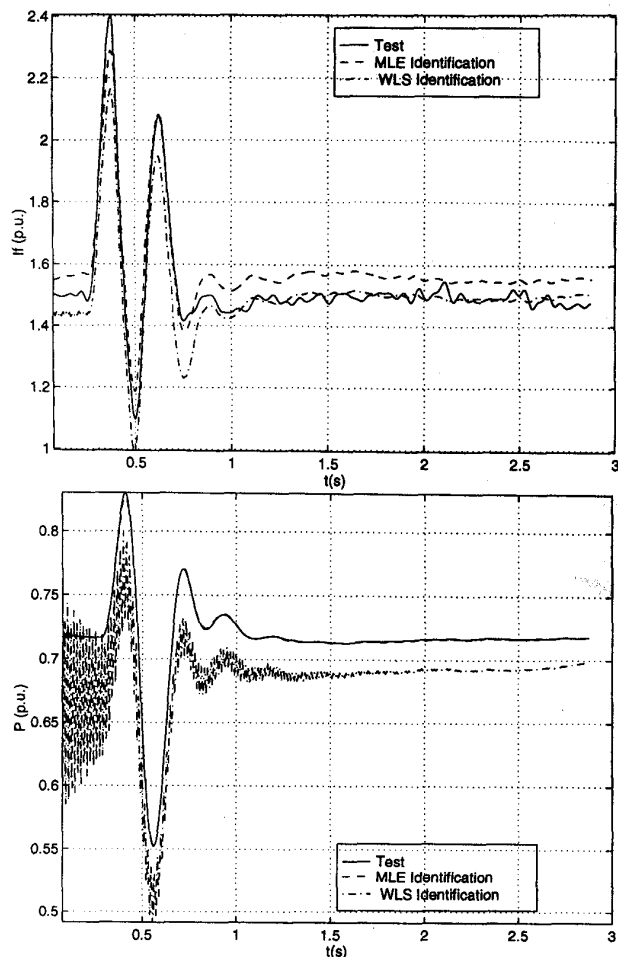


Fig. 8: Model cross-validation: field current, and active power.

VII. Conclusion

The present paper has attempted to apply the maximum-likelihood estimator in its original formulation to synchronous-machine parameter estimation. The proposed procedure, based on generalized least squares, is presented using large-disturbance response data. The results confirmed that the proposed maximum-likelihood estimates (MLE) are more consistent than the classical maximum-likelihood estimates which are equal to the weighted least-squares estimates (WLS). This work contributes to the clarification of some accepted concepts of the maximum-likelihood estimation method. It would be more interesting if the statistical inferences were done on the estimated parameters. Although the identification procedure uses on-line test data, the step response is known to be less more effective than PWM (pulse width modulated) or stochastic excitations and asymmetrical short-circuit tests in exciting all the machine modes. In near future, it is planned to conduct real modeling of synchronous machines from large-disturbance tests such as line-to-line short-circuits using the MLE.

VIII. References

- [1] I. Kamwa, P. Viarouge, E. J. Dickinson, "Identification of generalised models of synchronous machines from time-domain tests," *IEE Proc.-C*, **138**(6), pp.485-498, Nov. 1991.
- [2] R. Diggle, J. L. Dineley, "Generator Works Testing: Sudden Short-circuit or Standstill Variable Frequency-response Method," *IEE Proc.-C*, **128**(4), pp. 177-182, July 1981
- [3] H. Tsai, A. Keyhani, J. Demcko, R. G. Farmer, "On-Line Synchronous Machine Parameter Estimation from Small Disturbance Operating Data," *IEEE Trans.*, **EC-10**(1), 1995, pp. 25-35.
- [4] EPRI report EL-5736: "Confirmation of Test Methods for Synchronous Machine Dynamic Performance Models," Power Consumer Inc., Aug. 1988.
- [5] A. Keyhani, S. Hao, G. Dayal, "Maximum Likelihood Estimation of Solid-Rotor Synchronous Machine Parameters from SSFR Test Data," *IEEE Trans.*, **EC-4**(3), 1989, pp. 551-558.
- [6] M. L. Zhu, B. Mpanda-Mabwe, M. Crappe, M. Renglet, "Synchronous Machine Parameters Estimation Using Kalman Filter and Maximum Likelihood Combined Method," *Proc., Electrimsacs'96*, Vol. 1/3, September 1996, pp. 353-358.
- [7] R.E Maine, K. W. Iliff, "Formulation and Implementation of Practical Algorithm for Parameter Estimation with Process and Measurements noise," *SIAM J. Appl. Math.*, **41**(3), December 1981, pp.558-579.
- [8] J. Schoukens, R. Pintelon, *Identification of linear systems: A Practical Guideline to Accurate Modeling*, Pergamon Press.
- [9] R. K. Mehra, "On the Identification of Variances and Adaptive Kalman Filtering," *IEEE Trans. AC-15* (2), April 1970, pp. 175-184.
- [10] L. Ljung, T. Soderstrom, *Theory and Practice of Recursive Identification*, MIT Press, 1983.
- [11] A. A. F. Seber, C. J. Wild, *Nonlinear Regression*, John Wiley and Sons, New Zealand 1988.
- [12] G.C. Goodwin, R. L. Payne, *Dynamic System Identification: Experiment Design and Data Analysis*, Academic Press, New York, 1977.
- [13] C. K. Chui G. Chen, *Kalman Filtering with Real-Time Applications*, second edition, Springer-Verlag, Germany 1991.
- [14] R. Wamkeue, I. Kamwa, X. Dai-Do, "A Detailed Model of Grounded Synchronous Machines for Saturated Unsymmetrical Transients," *Proc. Electrimsacs'96*, Vol. 1/3, September 1996 pp. 333-340.
- [15] Andrew Grace, *Optimization Toolbox for use with matlab*, The MathWorks, Inc. Natick, Mass. 1992.
- [16] B. Paiement, "Identification des paramètres et des fonctions de transfert du système d'excitation," Report No. SEET- 93065, Service des Essais et Études techniques, Sept. 1993.
- [17] E. H. Watanabe, R. M. Stephan, M. Aredes, "New Concepts of Instantaneous Active and Reactive Powers in Electrical Systems with Generic Loads," *IEEE Trans.*, **PWRD-8**(2), April 1993, pp. 697-703.
- [18] L. Toivonene, J. Mörsky, "Digital Multirate Algorithms for Measurement of Voltage, Current, Power and Flicker," *IEEE Trans.*, **PWRD-10**(1), Jan. 1995, pp. 116-126.
- [19] P. Kundur, *Power System Stability and Control*, McGraw-Hill, 1994.
- [20] IEEE/ANSI Standard 115 (1996): Tests Procedures for Synchronous Machines.

- [21] P. C. Krause, O. Wasynczuz, S. D. Sudhoff, *Analysis of Electric Machinery*, IEEE Press, New York.
- [22] IEEE Guide for Synchronous Generator Modeling Practices in Stability Analysis, IEEE Std-1110, 1991.
- [23] I. Kamwa, M. Farzaneh, "Data Translation and Order Reduction for Turbine-Generator Models Used in Network Studies," *IEEE Trans. EC-12*(2), June 1997, pp. 118-126.
- [24] M. Salvatore, M. Savino, "Experimental Determination of Synchronous Machine Parameters," *IEE Proc. B*, **128** (4), pp.212-218, July 1981.
- [25] I. M. Canay, "Modelling of Alternating-Current Machines having Multiple Rotor Circuits," *IEEE Trans. EC-8*(2), June 1993, pp. 280-296.

IX. Appendix

$$x_{dd} = x_{md} + x_a = x_d; \quad x_{df} = x_{fd} = x_{D_1 d} = x_{d D_1} = x_{md} \quad (32)$$

$$x_{f D_1} = x_{D_1 f} = x_{D_1 D_k} = x_{D_k D_1} = x_{D_1 D_1} - x_{D_1} \quad (33)$$

$$x_{ff} = x_{md} + x_f + \sum_{i=1}^{nd} x_{kf_i} \quad (34)$$

$$x_{D_l D_l} = x_{md} + x_{D_l} + \sum_{i=1}^l x_{kf_i}; \quad l, k = 1 \dots nd \quad (35)$$

$$x_{qq} = x_{mq} + x_a = x_q; \quad x_{Q_l Q_l} = x_{Q_l} + x_{mq} \quad (36)$$

$$x_{q Q_l} = x_{Q_l q} = x_{Q_l Q_k} = x_{Q_k Q_l} = x_{mq}; \quad k, l = 1 \dots nq \quad (37)$$

$$\frac{di}{dt} = Ai + Bu; \quad y = Ci \quad (38)$$

$$B = \omega_n X^{-1}; \quad A = -B(R + \omega_m G) \quad (39)$$

$$i = [i_d, i_f, i_{D_1}, \dots, i_q, i_{Q_1}, \dots]^T; \quad y^T = [i_d, i_f, i_q] \quad (40)$$

$$R = \text{diag} [r_a, r_f, r_{D_1}, \dots, r_q, r_{Q_1}, \dots] \quad (41)$$

$$G = \begin{bmatrix} \ominus_{1, nd+2} & -G_q \\ \ominus_{nd+1, nd+2} & \ominus_{nd+1, nd+1} \\ -G_d & \ominus_{1, nd+1} \\ \ominus_{nq, nd+2} & \ominus_{nq, nq+1} \end{bmatrix} \quad (42)$$

$$X = \begin{bmatrix} X_d & \ominus_{nd+2, nq+1} \\ \ominus_{nq+1, nd+2} & X_q \end{bmatrix} \quad (43)$$

$$C = \begin{bmatrix} 1 & 0 & 0 & \ominus_{1, n-3} \\ 0 & 1 & 0 & \ominus_{1, n-3} \\ 0 & \ominus_{1, nd+2} & 1 & \ominus_{1, n-nd+3} \end{bmatrix} \quad (44)$$

$$X_d = \begin{bmatrix} x_{dd} & x_{df} & x_{d D_1} & \dots & x_{d D_{nd}} \\ x_{fd} & x_{ff} & x_{f D_1} & \dots & x_{f D_{nd}} \\ x_{D_1 d} & x_{D_1 f} & x_{D_1 D_1} & \dots & x_{D_1 D_{nd}} \\ \dots & \dots & \dots & \dots & \dots \\ x_{D_{nd} d} & x_{D_{nd} f} & x_{D_{nd} D_1} & \dots & x_{D_{nd} D_{nd}} \end{bmatrix} \quad (45)$$

$$X_q = \begin{bmatrix} x_{qq} & x_{q Q_1} & x_{q Q_2} & \dots & x_{q Q_{nq}} \\ x_{Q_1 q} & x_{Q_1 Q_1} & x_{Q_1 Q_2} & \dots & x_{Q_1 Q_{nq}} \\ x_{Q_2 q} & x_{Q_2 Q_1} & x_{Q_2 Q_2} & \dots & x_{Q_2 Q_{nq}} \\ \dots & \dots & \dots & \dots & \dots \\ x_{Q_{nq} q} & x_{Q_{nq} Q_1} & x_{Q_{nq} Q_2} & \dots & x_{Q_{nq} Q_{nq}} \end{bmatrix} \quad (46)$$

$$G_d = [x_{dd} \ x_{df} \ x_{d D_1} \ \dots \ x_{d D_{nd}}]; \quad G_q = [x_{qq} \ x_{q Q_1} \ x_{q Q_2} \ \dots \ x_{q Q_{nq}}] \quad (47)$$

X. Biographies

René Wamkeue received his B.Eng in Electrical Engineering in 1990 from University of Douala, Cameroon. From 1991 to 1992, he was employed as professor of Electrical Engineering at University of Douala. Since 1993, René Wamkeue has been enrolled as PhD candidate at École Polytechnique de Montréal. His research interest is in the control and modeling of electric machines and power electronics.

Innocent Kamwa has been with the Hydro-Québec research institute, IREQ, since 1988. He is an associate professor of Electrical Engineering at Laval University in Québec, Canada. His current interests involve the areas of synchronous-machine advancements, power system identification, monitoring and control. Kamwa received his B.Eng. and Ph.D. degrees in Electrical Engineering from Laval University in 1984 and 1988 respectively. He is a member a registered engineer in the province of Québec and a member of the Synchronous Machine and Stability Controls Subcommittees of the IEEE PES.

Xuan Dai-Do earned his BScA, MScA and PhD degrees in Electrical Engineering from Laval University, Québec, Canada in 1966, 1968 and 1971, respectively. He has been at Ecole Polytechnique de Montréal, Canada, since 1971, and is currently a Professor there. His areas of teaching and research are the analysis, modeling and simulation of HVAC and HVDC power systems. Dr. Do has authored or co-authored numerous technical papers. He is a Senior Member of IEEE and member of CIGRE. He was awarded the 1981 IEEE Outstanding Student Branch Counselor Award and IEEE Centennial Medal in 1984.

Ali Keyhani received his PhD from Purdue University, West Lafayette, Indiana in 1975. From 1967 to 1969, he worked for Hewlett-Packard Co. on the computer-aided design of electronic transformers. Currently, Dr. Keyhani is a Professor of Electrical Engineering at the Ohio State University, Columbus, Ohio. His research interest is in control and modeling, parameter estimation, failure detection of electric machines, transformers and drive systems.